

CLINICAL STUDY



# CXC chemokine receptor 7 ameliorates renal fibrosis by inhibiting $\beta$ -catenin signaling and epithelial-to-mesenchymal transition in tubular epithelial cells

Ping Meng<sup>a</sup>, Chunli Liu<sup>a</sup>, Jingchun Li<sup>a</sup>, Ping Fang<sup>b</sup>, Bo Yang<sup>c</sup>, Wei Sun<sup>a</sup> and Yunfang Zhang<sup>d</sup>

<sup>a</sup>Department of Central Laboratory, Huadu District People's Hospital of Guangzhou, Guangzhou, China; <sup>b</sup>Department of Laboratory Medicine, Huadu District People's Hospital of Guangzhou, Guangzhou, China; <sup>c</sup>Department of Clinical Nutrition, Huadu District People's Hospital of Guangzhou, Guangzhou, China; <sup>d</sup>Department of Nephrology, Huadu District People's Hospital of Guangzhou, Guangzhou, China

## ABSTRACT

Renal fibrosis is a common feature of various chronic kidney diseases. However, the underlying mechanism remains poorly understood. The CXC chemokine receptor (CXCR) family plays a role in renal fibrosis; however, the detailed mechanisms have not been elucidated. In this study, we investigated the potential role of CXCR7 in mediating renal fibrosis. CXCR7 expression is decreased in unilateral ischemia–reperfusion injury (UIRI) and unilateral ureteral obstruction mouse models. Furthermore, CXCR7 was specifically expressed primarily in the Lotus Tetragonolobus Lectin-expressing segment of tubules, was slightly expressed in the peanut agglutinin-expressing segment, and was barely expressed in the Dolichos biflorus agglutinin-expressing segment. Administration of pFlag-CXCR7, an overexpression plasmid for CXCR7, significantly inhibited the activation of  $\beta$ -catenin signaling and protected against the progression of epithelial-to-mesenchymal transition (EMT) and renal fibrosis in a UIRI mouse model. Using cultured HKC-8 cells, we found that CXCR7 significantly downregulated the expression of active  $\beta$ -catenin and fibrosis-related markers, including fibronectin, Collagen I, and  $\alpha$ -SMA. Furthermore, CXCR7 significantly attenuated TGF- $\beta$ 1-induced changes in  $\beta$ -catenin signaling, EMT and fibrosis. These results suggest that CXCR7 plays a crucial role in inhibiting the activation of  $\beta$ -catenin signaling and the progression of EMT and renal fibrosis. Thus, CXCR7 could be a novel therapeutic target for renal fibrosis.

## ARTICLE HISTORY

Received 4 May 2023  
Revised 26 December 2023  
Accepted 26 December 2023

## KEYWORDS

Chronic kidney diseases; renal fibrosis; CXCR7; EMT;  $\beta$ -catenin





## Introduction


Chronic kidney disease (CKD) is defined as chronic renal structural and functional impairment due to various causes (including a history of kidney damage greater than 3 months), including normal and abnormal pathological impairment of renal filtration rate (GFR), abnormal blood or urine composition, and imaging abnormalities for more than 3 months [1]. The impact of CKD on worldwide morbidity and mortality is rapidly increasing, indicating the shortcomings of therapeutic drugs at present. Hence, studies aimed at identifying therapeutic targets for CKD are desperately needed.

Renal fibrosis is a typical pathological change in CKD, is strongly associated with the deterioration of renal function and long-term prognosis in CKD patients and is characterized by abnormal deposition of extracellular matrix, gradual sclerosis of the renal parenchyma and scar formation to the point where the kidney completely loses its organ function.

EMT is an important biological process that contributes to renal fibrosis and CKD. The TGF- $\beta$ 1/Smad and Wnt/ $\beta$ -catenin signaling pathways are the major pathways involved in EMT [2]. Despite many attempts to block kidney fibrosis, few treatments have been approved for clinical practice, and a large treatment gap remains unknown [3]. Thus, novel antifibrotic therapies are urgently needed to prevent the progression of EMT and renal fibrosis in CKD patients.

Chemokine receptors are a family of GPCRs that respond to chemokines. These proteins are small, secreted proteins with molecular weights in the range of 8 to 12 kDa that are involved mainly in the regulation of immune cell recruitment. Subsequently, their role has been extended to other pathological and physiological conditions, including embryogenesis, angiogenesis, hematopoiesis, atherosclerosis, tumor growth, and metastasis, and they function as coreceptors for several human immunodeficiency virus strains [4]. Changes in chemokine levels and in the expression of chemokine

**CONTACT** Wei Sun  [mengnini@smu.edu.cn](mailto:mengnini@smu.edu.cn)  Department of Central Laboratory, Huadu District People's Hospital of Guangzhou, Guangzhou, China; Yunfang Zhang  [zhang\\_yunf@163.com](mailto:zhang_yunf@163.com)  Department of Nephrology, Huadu District People's Hospital of Guangzhou, Guangzhou, China.

 Supplemental data for this article can be accessed online at <https://doi.org/10.1080/0886022X.2023.2300727>.

© 2024 The Author(s). Published by Informa UK Limited, trading as Taylor & Francis Group

This is an Open Access article distributed under the terms of the Creative Commons Attribution-NonCommercial License (<http://creativecommons.org/licenses/by-nc/4.0/>), which permits unrestricted non-commercial use, distribution, and reproduction in any medium, provided the original work is properly cited. The terms on which this article has been published allow the posting of the Accepted Manuscript in a repository by the author(s) or with their consent.

receptors at lesion sites are also important components of renal fibrosis [5]. Thus, investigations of the role of CXCRs in the process of renal fibrosis are urgently needed.

During EMT and renal fibrosis, many chemokines and their receptors are crucial players in this process. A previous study showed that high expression of CXCR2 was strongly associated with the Wnt/ $\beta$ -catenin signaling pathway and renal fibrosis. Moreover, blockade of CXCR2 protects renal function, inhibits the Wnt/ $\beta$ -catenin signaling pathway and reduces renal fibrosis [6–8]. High expression levels of CXCR4 have been reported in glomerular and tubular cells independent of the progression of renal fibrosis [9–11]. Evidence indicates that CXCR6 plays an important role in Ang II-induced renal injury and fibrosis [12,13]. Accumulating evidence indicates that chemokine receptors are key regulators of renal fibrosis in diseased kidneys. However, the mechanisms by which chemokine receptors modulate renal fibrosis have not been fully elucidated.

CXCR7, also known as a typical chemokine receptor 3 (ACKR3), is not a classic seven transmembrane-spanning receptor and therefore belongs to the class of ACKRs expressed in monocytes, endothelial cells, B cells, and cardiomyocytes. CXCR7 has previously been reported to be involved in physiological and pathophysiological processes such as cancer, coronary artery disease, stroke, inflammatory conditions, and HIV infection [14,15]. Recently, CXCR7 was found to control cell adhesion and migration by regulating EMT [16,17]. Another report showed that activation of CXCR7 can override the fibrotic activity of macrophages to reduce JAG1 expression in PCECs and subsequent lung fibrosis [18]. CXCR7 has been discovered to be a novel small-molecule modulator that can treat cardiac fibrosis [19]. It has also been reported that overexpressed CXCR7 might inhibit fibrosis *via* the Wnt/ $\beta$ -catenin pathway during angiogenesis in human umbilical vein endothelial cells [20]. Thus, CXCR7 seems to be closely associated with fibrotic disease. To date, relatively little is known about the role of CXCR7 in renal fibrosis.

In this study, we investigated CXCR7 expression and localization and revealed the contribution of CXCR7 to the regulation of  $\beta$ -catenin signaling, EMT and renal fibrosis *in vivo* and *in vitro*. These results suggest that CXCR7 could be a new target for mitigating renal fibrosis.

## Materials and methods

### Animal models and treatments

The unilateral ureteral obstruction (UUO) mouse model was described previously [21]. Six- to eight-week-old male C57BL/6 mice (22–24 g) were generated by ligating the left ureter. After 7 days, renal tissue samples were collected from the mice for analysis. Two groups of mice were used: (1) Sham control ( $n=5$ ) and (2) UUO mice ( $n=5$ ).

The UIRI mouse model was generated in C57BL/6 male mice according to an established protocol. First, the left renal pedicle was clipped with a microaneurysm clamp

(item no. 18051–35; Fine Science Tools, Cambridge, UK). Throughout the process of ischemia, the mouse body temperature was controlled between approximately 37°C and 38°C through a metal bath system. After removing the microaneurysm clamps, reperfusion of the left ischemic kidney was visually confirmed. Ten days later, the whole right kidney was excised under sterile conditions. One day later, serum, urine and left renal tissue samples were collected for analysis. Two groups of mice were used: (1) Sham control ( $n=5$ ) and (2) UIRI mice ( $n=5$ ).

For the CXCR7-overexpressing UIRI mouse model, three groups of mice were used: (1) Sham control ( $n=5$ ), (2) UIRI mice rapidly injected with a large volume of the pcDNA3 plasmid *via* the tail vein as previously reported ( $n=5$ ), and (3) UIRI mice injected with the pFlag-CXCR7 plasmid *via* the tail vein ( $n=5$ ). All mice were kept in a room maintained at an appropriate temperature and humidity on a 12h light/dark cycle and were provided ample food and water. All the experiments were performed according to the Guidelines for the Care and Use of Laboratory Animals. The animal ethics approval number was MDL2023-04-08-01.

### Histology staining

Paraffin-embedded mouse kidney sections were prepared by a routine procedure. Periodic acid-Schiff (PAS) staining was performed on paraffin-embedded kidney sections (3  $\mu$ m) to determine the morphology of renal tubules according to the manufacturer's instructions (PAS Staining Kit, C01425-3, Beyotime). Sections (3  $\mu$ m) were subjected to Masson staining to assess collagen deposition and fibrotic lesions according to the manufacturer's instructions (Masson's Trichrome Stain Kit, G1340, Solarbio). Sirius red staining was performed on paraffin-embedded kidney sections (6  $\mu$ m) to determine the distribution of collagen according to the manufacturer's instructions (Sirius Red Stain Kit, DC0040; Leagene).

### Cell culture and treatment

Human proximal tubular epithelial (HKC-8) cells were cultured as previously described [7]. HKC-8 cells were stimulated with recombinant human TGF- $\beta$ 1 protein (R&D Systems, Minneapolis, MN) (5 ng/ml). To upregulate CXCR7 expression in HKC-8 cells, a plasmid encoding overexpressed CXCR7 was constructed by cloning the CXCR7 gene into the NotI and XhoI sites on the pcDNA3.1-3 x Flag-C vector. The CXCR7 cDNA was amplified using the following primers: forwards primer 5'-3' GACGAT GACAAGCTTGCGGCCGCCATGGATCTGCATCTCTTCGAC and reverse primer 5'-3' GGTACCTCATCTAGACTCGAGTCATTGGT GCTCTGCTCC. A control plasmid (pcDNA3) or CXCR7 expression plasmid (pFlag-CXCR7) was also transfected into HKC-8 cells using Lipofectamine 2000 (Life Technologies, Carlsbad, CA) according to the manufacturer's instructions. After transfection for 24h, the efficacy of the various treatments was determined by quantitative real-time PCR, Western blotting, and immunostaining.

### RNA isolation and qRT-PCR analysis

Total RNA was extracted from kidney tissue or HKC-8 cells using TRIzol reagent (Life Technologies, Grand Island, NY). After isolation, single-stranded cDNA was generated from 1 µg of total RNA *via* reverse transcription by using a superscript reverse transcriptase kit (R333-01, Vazyme) according to the manufacturer's instructions. Quantitative real-time PCR was performed using Taq Pro Universal SYBR qPCR Master Mix (Q712-02, Vazyme). The detection of cDNA expression of the specific genes was performed with an ABI PRISM 7000 instrument (Applied Biosystems, Foster City, CA). The mRNA expression levels of various genes were calculated after normalization to that of  $\beta$ -actin. All primers used in qRT-PCR are displayed in Table S1.

### Serum creatinine (Scr) and blood urea nitrogen (BUN) assays

The levels of Scr and BUN in the UIRI model animals were determined by an automatic chemical analyzer (AU480 Chemistry Analyzer, Beckman Coulter, Atlanta, Georgia). The level of Scr or BUN was expressed as mg/dl.

### Western blot analysis

Protein expression was analyzed by western blot (WB) analysis as described previously [7]. The following primary antibodies were used: anti-fibronectin (F3648; Sigma-Aldrich), anti-active- $\beta$ -catenin (19807T; Cell Signaling Technology), anti- $\beta$ -catenin (610154; BD Biosciences), anti-CXCR7 (SAB2700198; Sigma), anti- $\alpha$ -SMA (ab5694; Abcam), anti-Collagen I (ab34710; Abcam), anti-vimentin (SAB1305447, Sigma-Aldrich), anti-snail1 (ab180714; Abcam), anti-E-cadherin (3195; Cell Signaling Technology), anti- $\alpha$ -tubulin (RM2007; Ray Antibody Biotech, Beijing, China), anti-GAPDH (RM2001; Ray Antibody Biotech), and anti-flag-tag (KM3002; Sungene Biotech Co.).

### Immunohistochemical staining

Mouse kidneys were promptly perfused with 4% paraformaldehyde and fixed in paraffin for sectioning after removal. Three-micron-thick kidney sections were mounted for immunohistochemical staining. Cells that had grown on glass coverslips were fixed with 4% paraformaldehyde for 10 min at room temperature. Then, the cells were treated with 5% Triton for 30 min. Primary antibodies were incubated at 4°C overnight. The next day, the tissues and cells were incubated with secondary antibodies under the guidance of the immunohistochemical staining protocol. The antibodies used were as follows: anti-CXCR7 (SAB2700198, Sigma), anti-fibronectin (F3648; Sigma-Aldrich), anti- $\alpha$ -SMA (ab5694; Abcam), and anti- $\beta$ -catenin (610154; BD Biosciences, ab15180; Abcam). The secondary antibodies used were as follows: AffiniPure donkey anti-rabbit IgG (H+L) (711-005-152; Jackson ImmunoResearch) and AffiniPure donkey anti-mouse IgG (H+L) (711-005-150; Jackson ImmunoResearch). DAB (SK-4100) and AEC (SK-4200) substrate kits were obtained

from Vector Laboratories. An Olympus microscope was used to observe and photograph the sections.

### Immunofluorescence staining

Fixed kidneys were embedded in snap-frozen OCT compound. Three-micron-thick kidney sections were mounted for immunofluorescence staining. Frozen kidney sections were blocked with 5% donkey serum and incubated with primary antibodies at 4°C overnight. After the sections were washed with TBST and incubated with fluorescent dye-conjugated secondary antibodies (Jackson Immuno-Research Laboratories, West Grove, PA), nuclear staining was performed using DAPI (Sigma-Aldrich) according to the manufacturer's specifications. Cells that had grown on glass coverslips were fixed with 4% paraformaldehyde for 10 min and treated with 0.2% Triton for 10 min at room temperature. Primary antibodies were incubated at 4°C overnight. The next day, tissue and cell immunofluorescence staining was performed following the routine protocol. The primary antibodies used were as follows: anti-fibronectin (F3648; Sigma-Aldrich), anti-F4/80 (GB2108010C; Servicebio), anti-CD31 (ab28364; Abcam), anti-CXCR7 (MAB42274; R&D Systems), anti-CXCR7 (GTX638193; GeneTex), anti-Lotus Tetragonolobus Lectin (FL-1321; VECTOR Laboratories), anti-Peanut Agglutinin (FL-1071; VECTOR Laboratories), and anti-Dolichos Biflorus Agglutinin (FL1031; VECTOR Laboratories). The secondary antibodies used were as follows: goat anti-mouse IgG H&L (Alexa Fluor® 647) (ab150115; Abcam), goat anti-mouse IgG H&L (Alexa Fluor® 488) (ab150113; Abcam), goat anti-rabbit IgG H&L (Alexa Fluor® 488) (ab150077; Abcam), and goat anti-rabbit IgG H&L (Alexa Fluor® 647) (ab150083; Abcam). The nuclei were stained with DAPI (C1006; Beyotime). Laser confocal microscopy was used for observation and imaging (Leica Application Suite X).

### Statistical analysis

All the data examined are expressed as the mean  $\pm$  SEM. All the statistical analyses were performed using GraphPad Prism version 9.5 software. Comparisons between two groups were analyzed using a t test. Comparisons among multiple groups were performed by one-way ANOVA.  $p < 0.05$  was considered to indicate statistical significance.

## Results

### CXCR7 is downregulated in renal tubule cells of mice with CKD

To investigate CXCR7 regulation, we used UIRI and UO mouse models to examine the expression of CXCR7 in the kidney. As shown in Figure 1A, the mRNA level of CXCR7 was lower in the UIRI model than in the control group. In parallel, we examined the protein level of CXCR7 *via* WB. The results showed that the protein expression of CXCR7 was downregulated, as fibrosis-related fibronectin (FN) was upregulated in the UIRI model compared to the control (Figure 1B–D).

Furthermore, immunohistochemical staining for CXCR7 also indicated that CXCR7 expression was lower in the renal tubules of the UIRI model mice than in those of the control mice (Figure 1E). Similarly, the mRNA level of *CXCR7* was lower in the UUO model than in the control group (Figure 1F). Analysis of WB and immunohistochemical staining also

showed that the expression of CXCR7 was downregulated in the renal tubules of the UUO model mice compared to those of the control rats (Figure 1G–J). These results indicate that the expression of CXCR7 was decreased in CKD model mice compared to that in controls, suggesting a potential role for CXCR7 in mediating tubular injury and renal fibrosis.

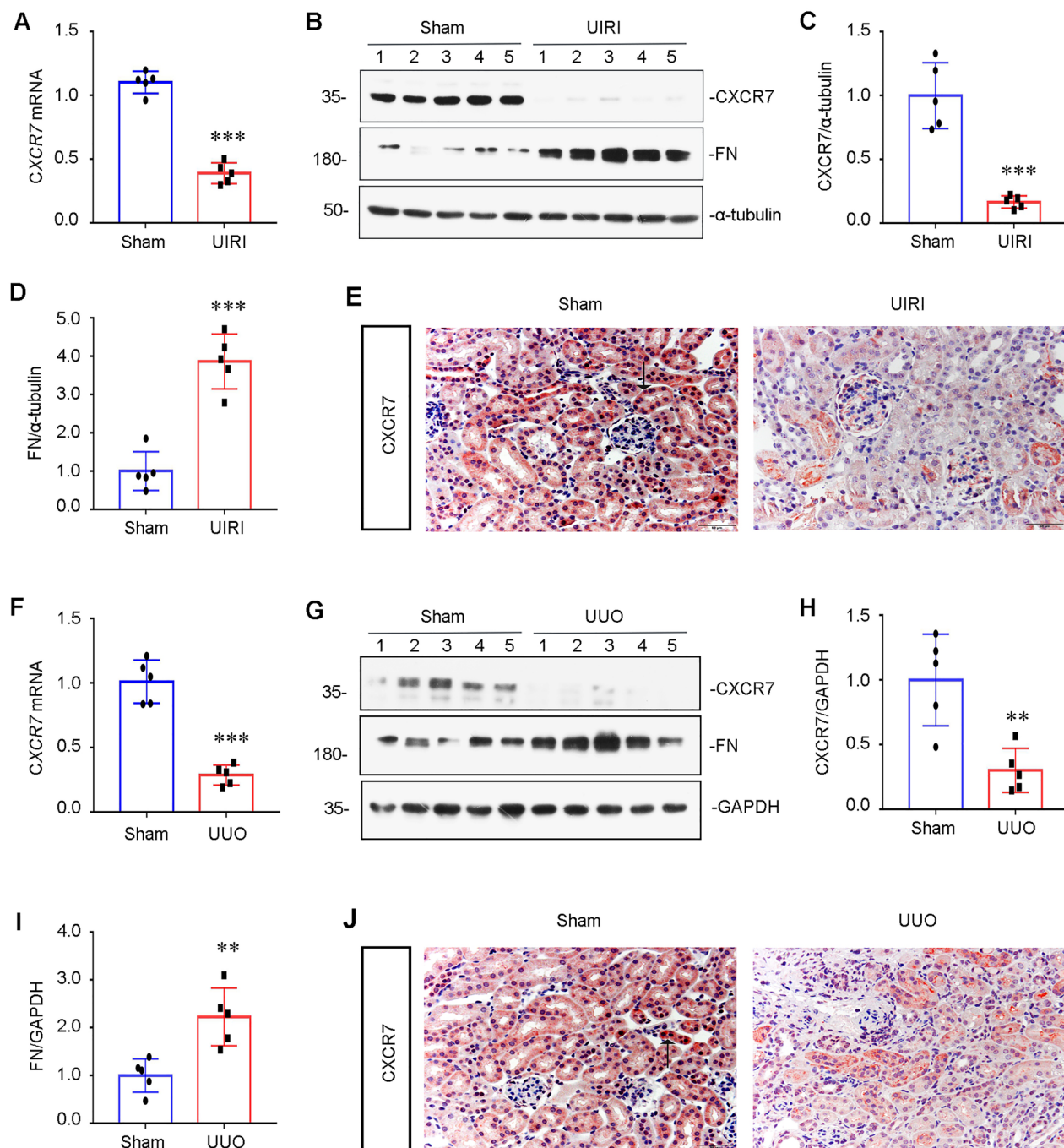


**Figure 1.** CXCR7 expression is downregulated in renal tubular cells.

(A) Graphical representations showing the relative abundance of *CXCR7* mRNA in the UIRI mouse model. \*\*\* $P < 0.001$ .  $n = 5$ . (B) Representative Western blots showing renal expression of CXCR7 and FN in the two groups, as indicated. (C–D) Graphical representations of (C) CXCR7 and (D) FN protein expression levels are shown. \*\*\* $P < 0.001$ .  $n = 5$ . (E) Immunohistochemical staining showing the expression of CXCR7 in the UIRI mouse model. Arrows indicate positive staining. Scale bar, 50  $\mu\text{m}$ . (F) Graphical representations showing the relative abundance of *CXCR7* mRNA in the UUO mouse model. \*\*\* $P < 0.001$ .  $n = 5$ . (G) Representative Western blots showing renal expression of CXCR7 and FN in UUO model mice, as indicated. (H–I) Graphical representations of (H) CXCR7 and (I) FN protein expression levels are shown. \*\* $P < 0.01$ .  $n = 5$ . (J) Immunohistochemical staining showing the expression of CXCR7 in UUO model mice. Arrows indicate positive staining. Scale bar, 50  $\mu\text{m}$ .



To determine the exact location of CXCR7 in renal tubules, we used immunofluorescence staining to detect CXCR7 *via* markers of specific segments of the renal tubules in the UIRI model. As shown in [Figure 2A](#), CXCR7 was largely colocalized with lotus tetragonolobus lectin, a proximal tubule marker and was less highly expressed with peanut agglutinin, a distal tubule marker; however, it was barely expressed with dolichos biflorus agglutinin, a collecting duct marker. Neither CXCR7 nor the macrophage marker F4/80 was expressed on the macrophages ([Figure 2B](#)). In addition, we stained for CXCR7 with the endothelial cell marker CD31. As shown in [Figure 2C](#), CXCR7 was partly expressed in endothelial cells and mostly expressed in tubular epithelial cells. Based on these results, we postulated that CXCR7 was largely expressed in renal tubule cells.

### Induction of CXCR7 inhibits renal fibrosis and $\beta$ -catenin signaling after UIRI

To examine whether CXCR7 can influence renal fibrosis, we assessed whether pFlag-CXCR7-mediated overexpression of CXCR7 occurred *via* vein injection in the UIRI mouse model ([Figure 3A](#)). One day after injection of the pFlag-CXCR7 plasmid vector, the mRNA and protein levels of CXCR7 tended to increase. Three days later, the concentration of CXCR7 reached its maximum. Even 5 and 7 days after the injection, CXCR7 expression was still high ([Supplemental Figure S1A–C](#)). Neither the overexpression of CXCR7 with the pFlag-CXCR7 plasmid nor the control treatment had no effect on renal fibrosis in sham mice ([Supplemental Figure S1D–G](#)). Scr and BUN levels were increased in UIRI mice but inhibited after CXCR7 was overexpressed ([Figure 3B and C](#)). Notably, the mRNA level of CXCR7 was recovered after the tail vein injection of pFlag-CXCR7 into UIRI mice ([Figure 3D](#)). To verify the overexpression effect of the CXCR7 plasmid, we detected the expression of CXCR7 and the Flag tag. As shown in [Figure 2E, F](#), the protein levels of CXCR7 and Flag were upregulated in pFlag-CXCR7-mediated UIRI mouse kidney tissues. In addition, the immunofluorescence staining results also indicated that CXCR7 was mostly located in tubular cells and was downregulated in the UIRI model and upregulated by pFlag-CXCR7 overexpression ([Figure 3G](#)). We then performed PAS staining to reveal damaged tubules by revealing the morphology of the tubules. PAS staining revealed that overexpression of CXCR7 protected against tubular injury in UIRI mice ([Figure 3G](#)). These results indicated that the induction of CXCR7 expression could improve renal function and protect against tubular injury after UIRI.

After further exploring the protective role of CXCR7 in UIRI, we found that the protein levels of Collagen I and FN were significantly decreased after the overexpression of CXCR7 in UIRI mice ([Figure 4A–C](#)). Next, we assessed E-cadherin and  $\beta$ -catenin signaling, which are closely related to renal fibrosis. WB analysis also revealed that the expression of E-cadherin was recovered and that the expression of active  $\beta$ -catenin was significantly inhibited after CXCR7 activation in UIRI mice ([Figure 4A, D and E](#)). The mRNA levels of *Collagen I*

and  $\alpha$ -SMA were also downregulated after CXCR7 activation in UIRI mice ([Figure 4F and G](#)). Furthermore, consistent results were found by Masson trichrome (MASSON) staining, Sirius Red staining, and FN immunostaining ([Figure 4H](#)). We also determined the expression of  $\beta$ -catenin by immunostaining. Similar results were observed when  $\beta$ -catenin was visualized by immunostaining ([Figure 4H](#)). Thus, overexpression of CXCR7 could abrogate renal fibrosis *via*  $\beta$ -catenin signaling in the UIRI model.

### Activation of CXCR7 inhibits renal fibrosis and the $\beta$ -catenin signaling pathway *in vitro*

Next, we sought to define the molecular mechanisms involved in the downregulation of CXCR7 in HKC-8 cells. CXCR7 expression was induced by transfecting HKC-8 cells with pFlag-CXCR7. As shown in [Figure 5A](#), the mRNA level of CXCR7 was significantly increased after pFlag-CXCR7 transfection. The mRNA levels of fibrosis-related markers, including  $\alpha$ -SMA, FN and *Collagen I*, were also decreased ([Figure 5B–D](#)). Furthermore, we examined the protein levels by WB analysis. Compared to that in the pcDNA3 control, the Flag protein (tagged with pFlag-CXCR7) was significantly expressed after pFlag-CXCR7 transfection ([Figure 5E](#)). The protein expression level of CXCR7 was also drastically upregulated ([Figure 5E and F](#)). CXCR7 also inhibited the expression of FN and  $\beta$ -catenin *in vitro* ([Figure 5E, G, and H](#)).

### CXCR7 inhibits TGF- $\beta$ 1-induced $\beta$ -catenin signaling, EMT and fibrogenesis in HKC-8 cells

To further confirm the role of CXCR7 in mediating fibrosis, we determined the role of CXCR7 in TGF- $\beta$ 1-induced renal fibrosis in HKC-8 cells. TGF- $\beta$ 1 modulates a major fibrogenic factor [22]. We first determined the expression of Flag, FN and  $\alpha$ -SMA in HKC-8 cells transfected with pFlag-CXCR7 and induced by TGF- $\beta$ 1 expression. The FLAG tag was successfully expressed by plasmid transfection ([Figure 6A](#)). As shown in [Figure 6A–C](#), CXCR7 largely inhibited the upregulation of FN and  $\alpha$ -SMA induced by TGF- $\beta$ 1 in CXCR7-overexpressing cells. The mRNA level of CXCR7 was recovered in the TGF- $\beta$ 1-induced CXCR7-overexpressing cells ([Figure 6D](#)). In addition, the mRNA levels of *Collagen I* and FN were downregulated in CXCR7-overexpressing cells ([Figure 6E and F](#)). Immunofluorescence staining also indicated that overexpression of CXCR7 markedly reduced the expression of FN ([Figure 6G](#)). These results indicated that CXCR7 inhibited TGF- $\beta$ 1-induced fibrogenesis *in vitro*.

To determine how CXCR7 inhibits TGF- $\beta$ 1-induced renal fibrosis, we further explored  $\beta$ -catenin signaling *in vitro*. As shown in [Figure 7A and B](#), overexpression of CXCR7 significantly inhibited the upregulation of active  $\beta$ -catenin. Interestingly, we found that the expression of the EMT-related proteins E-cadherin, Vimentin, and Snail1 was greatly decreased following transfection with the CXCR7 expression plasmid compared to that in the pcDNA3 group ([Figure 7A, C–E](#)). Immunostaining showed that CXCR7 inhibited the

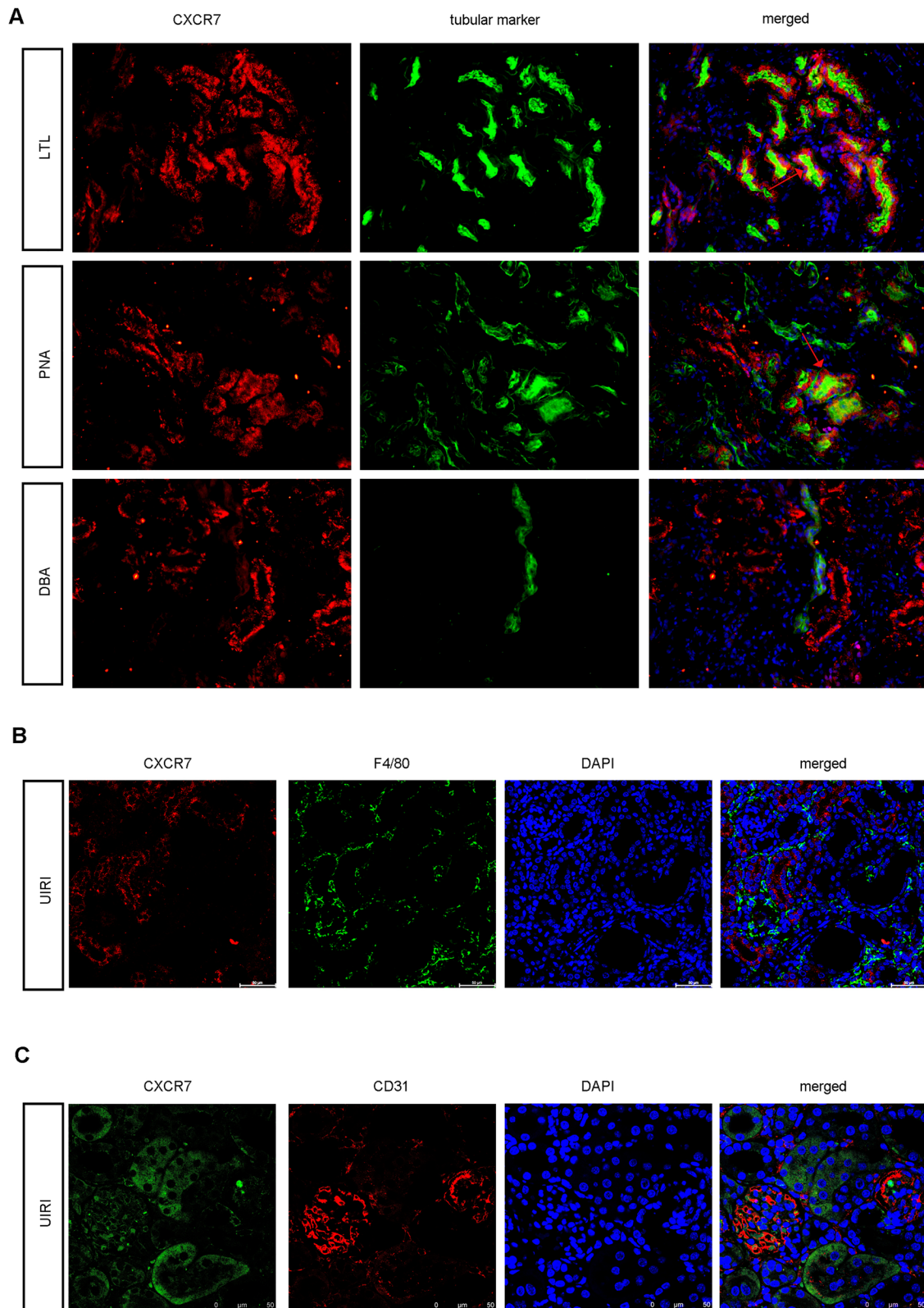


**Figure 2.** CXCR7 is expressed mainly in renal tubule epithelial cells.

(A) Images of CXCR7 and various segment-specific tubular marker colocalization in the kidneys of sham mice. Frozen kidney sections (3  $\mu\text{m}$ ) were collected from the sham mice. CXCR7 (red) and three segment-specific tubular markers (green), namely, lotus tetragonolobus lectin (LTL), peanut agglutinin (PNA), and dolichos biflorus agglutinin (DBA), were detected by immunofluorescence. Scale bar, 50  $\mu\text{m}$ . (B) Immunofluorescence staining for CXCR7 (red) and F4/80 (green) and DAPI staining were performed on the kidneys of UIRI mice. Scale bar, 50  $\mu\text{m}$ . (C) Immunofluorescence staining of CXCR7 (green) and CD31 (red) was performed, and immunofluorescence was used to detect DAPI in the kidneys of the UIRI model mice. Scale bar, 50  $\mu\text{m}$ .

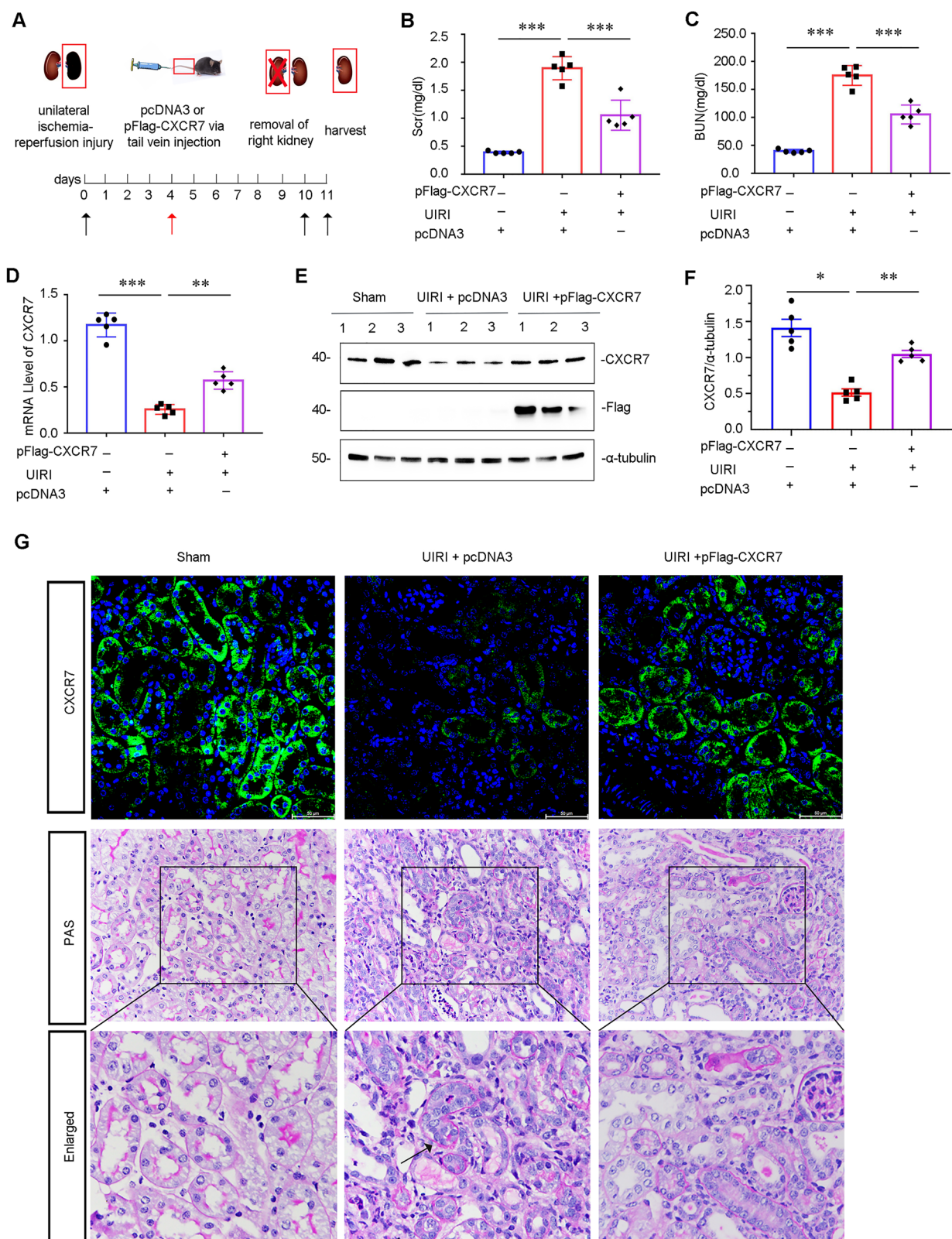


**Figure 3.** Overexpression of CXCR7 protects against renal dysfunction *in vivo*.

(A) Experimental design. The black arrows indicate the timing of renal UIRI surgery. Red arrows indicate the injection of pcDNA3 or the pFlag-CXCR7 plasmid via the tail vein. (B) Scr and (C) BUN levels in the three groups. \*\*\* $P < 0.001$ .  $n = 5$ . (D) Graphical representations showing the relative abundance of CXCR7 mRNA in the three groups. (E) Protein expression levels of Flag and CXCR7; graphical representations showing the relative abundance of the CXCR7 protein in the three groups (F). \* $P < 0.05$ .  $n = 5$ . (G) Representative images showing CXCR7 (green) and PAS staining in the three groups. Boxed areas are enlarged in the bottom panels. Arrows indicate the injured tubules. Scale bar, 50  $\mu\text{m}$ .



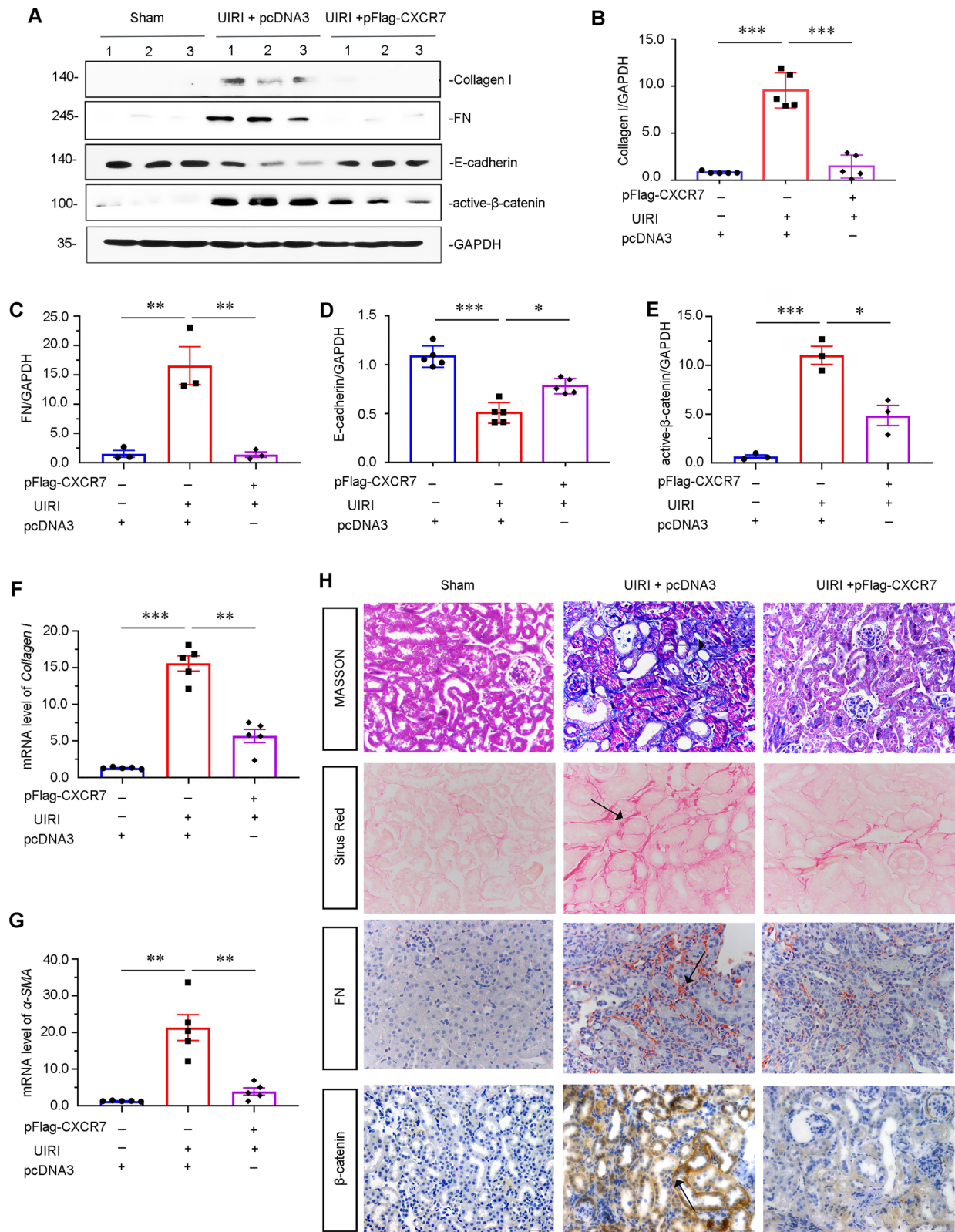


**Figure 4.** CXCR7 inhibits renal fibrosis through  $\beta$ -catenin signaling in the UIRI mouse model. (A) Representative protein graphs and expression levels of (B) Collagen I, (C) FN, (D) E-cadherin, and (E) active  $\beta$ -catenin are shown.  $*P < 0.05$ ,  $**P < 0.01$ ,  $***P < 0.001$ .  $n = 5$ . (F–G) Graphical representations showing the relative abundance of *Collagen I* and  *$\alpha$ -SMA* mRNA in the three groups.  $**P < 0.01$ ,  $***P < 0.001$ .  $n = 3$ . (H) Representative micrographs showing Masson, Sirius Red pathological, FN and  $\beta$ -catenin immunohistochemical staining in the three groups, as indicated. Arrows indicate positive staining. Scale bar,  $50\ \mu\text{m}$ .



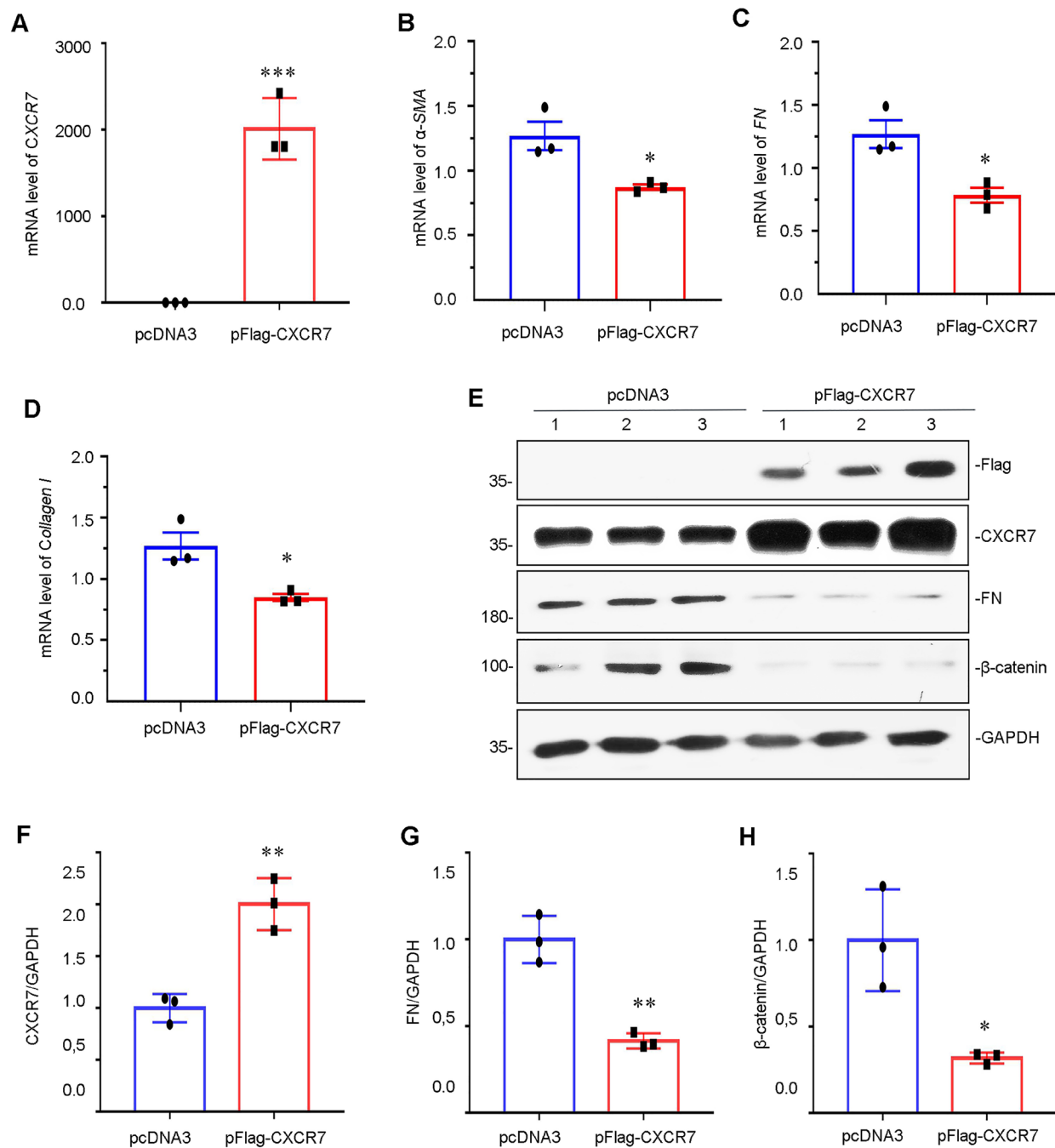


**Figure 5.** Overexpression of CXCR7 inhibits FN and  $\beta$ -catenin expression.

(A–D) Graphical representations showing the relative mRNA levels of *CXCR7*,  *$\alpha$ -SMA*, *FN* and *Collagen I* versus those in the pcDNA3 group. \* $P < 0.05$ , \*\*\* $P < 0.001$ .  $n = 3$ . (E) Representative micrographs of WB and quantitative statistical data showing the protein levels of (F) CXCR7, (G) FN and (H)  $\beta$ -catenin in each group. \* $P < 0.05$ , \*\* $P < 0.01$ .  $n = 3$ .

activation of  $\beta$ -catenin in TGF- $\beta$ 1-treated HKC-8 cells (Figure 7F). Thus, these results clarify that CXCR7 plays a key role in  $\beta$ -catenin signaling, EMT and fibrosis in renal tubular epithelial cells.

## Discussion

Renal fibrosis is involved in the progression of various CKDs [23]. Previous studies have shown that the CXCR

family of proteins plays a critical role in renal fibrosis [12]. However, little is known about whether CXCR7 is involved in the regulation of renal fibrosis. In our study, we first reported that CXCR7 was related to renal fibrosis. We first assessed the expression of CXCR7 in experimental UUO and UIRI mouse models. The results showed that CXCR7 was downregulated predominantly in injured tubular cells (Figures 1 and 2). Our pilot study showed that CXCR7 might be involved in renal fibrosis. Furthermore,

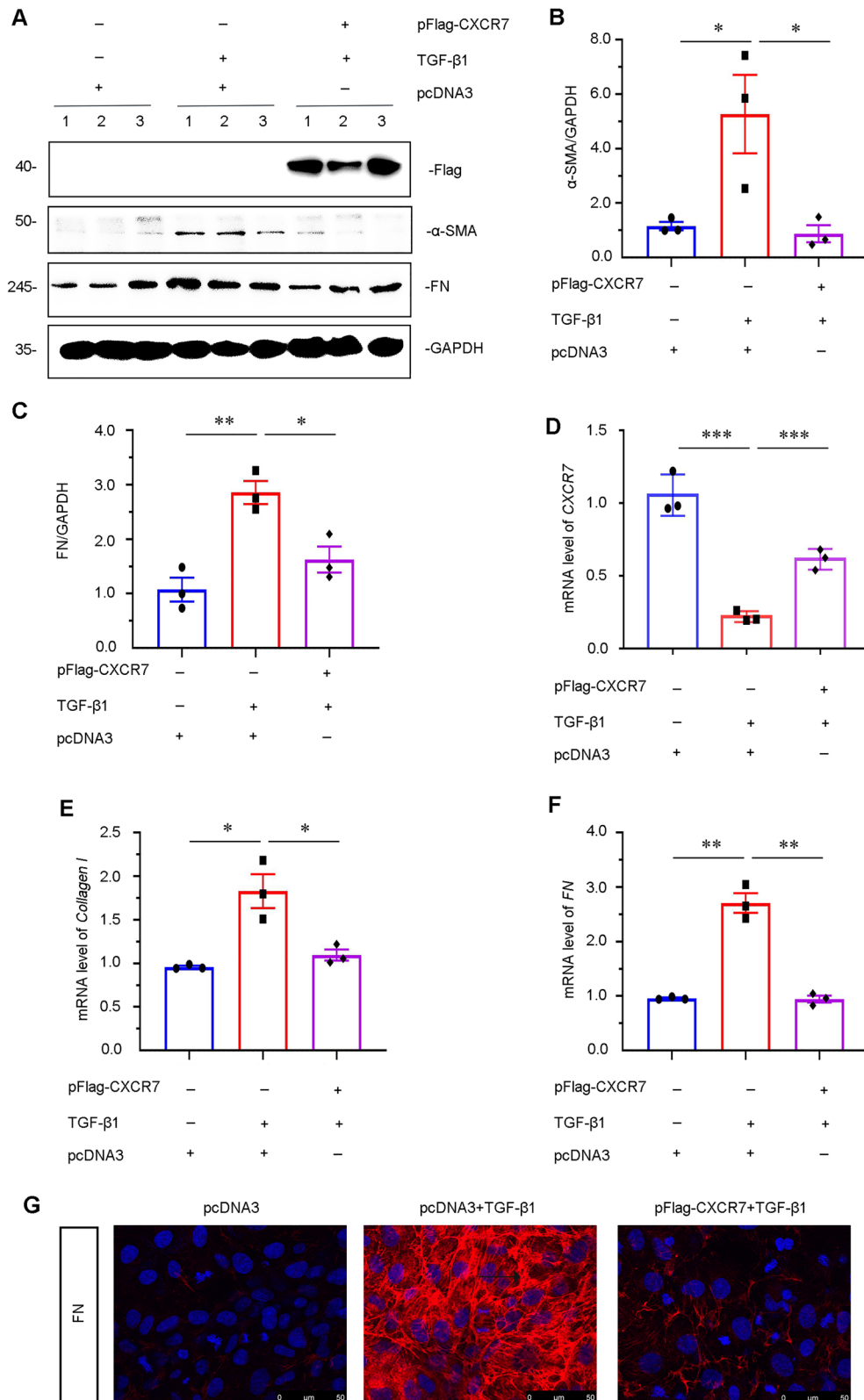


**Figure 6.** CXCR7 inhibits fibrogenesis in TGF-β1-treated tubular cells *in vitro*. (A) Representative micrographs of WB and quantitative statistical data showing the protein levels of (B) α-SMA and (C) FN in each group. \* $P < 0.05$ , \*\* $P < 0.01$ ,  $n = 3$ . (D–F) Graphical representations showing the relative mRNA levels of *CXCR7*, *Collagen I* and *FN* in the different groups. \* $P < 0.05$ , \*\* $P < 0.01$ , \*\*\* $P < 0.001$ ,  $n = 3$ . (G) Representative micrographs showing the protein expression level of FN in each group, as indicated. Frozen sections were stained with FN antibodies. Scale bar, 50 μm.

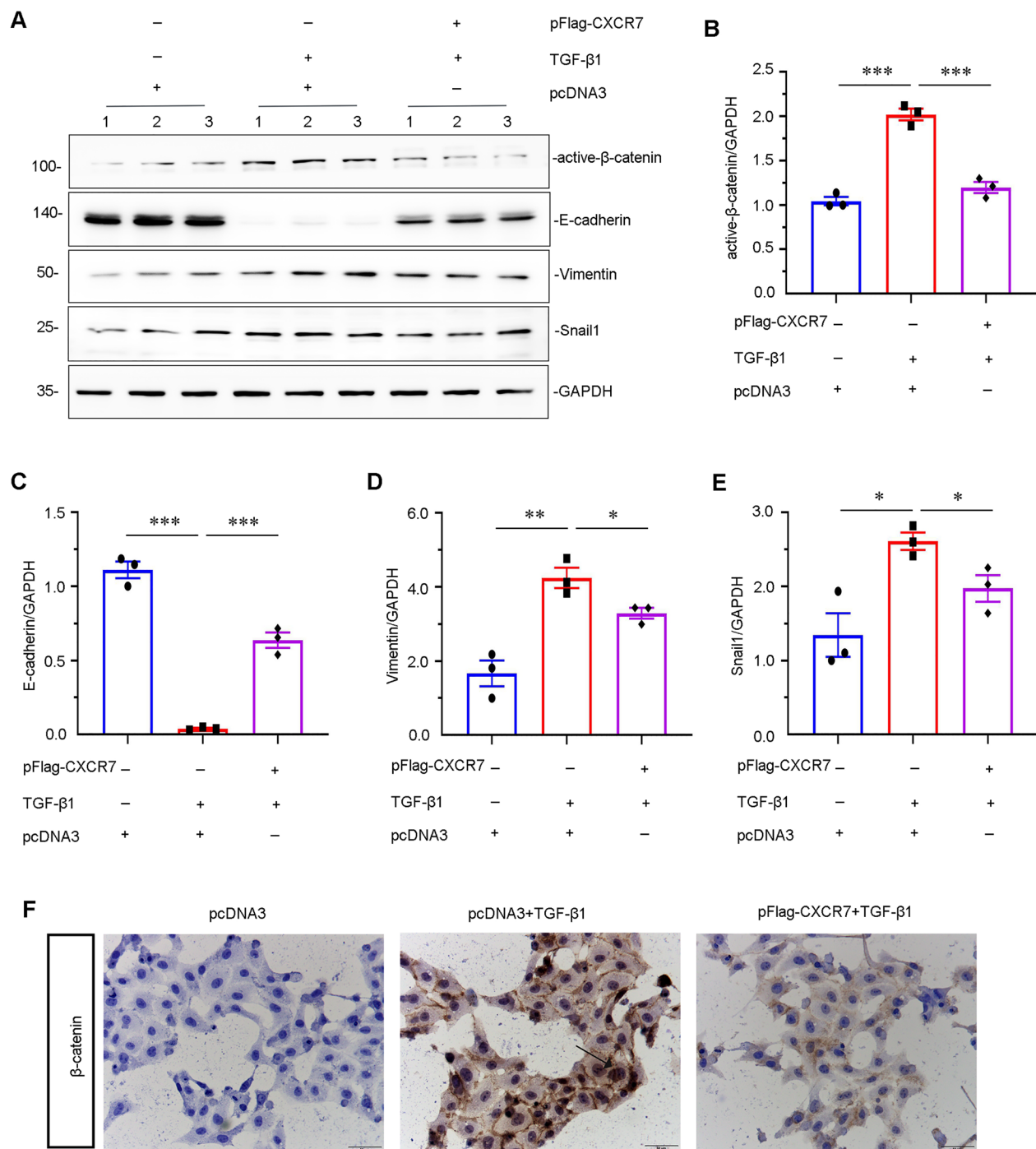


**Figure 7.** CXCR7 inhibits EMT and  $\beta$ -catenin signaling in TGF- $\beta$ 1-treated tubular cells *in vitro*. (A) Representative micrographs of WB and quantitative statistical data showing the protein levels of (B) active  $\beta$ -catenin, (C) E-cadherin, (D) vimentin, and (E) Snail1 in each group. \* $P < 0.05$ , \*\* $P < 0.01$ , \*\*\* $P < 0.001$ .  $n = 3$ . (F) Representative cell slime immunohistochemical staining showing the protein expression level of  $\beta$ -catenin in each group, as indicated. Arrows indicate positive staining. Scale bar, 50  $\mu$ m.

overexpression of CXCR7 effectively protected renal function and weakened renal fibrosis *in vivo* and *in vitro* (Figures 3, 4, 5 and 6). As such, we hypothesized that CXCR7 orchestrates renal fibrosis. However, the mechanism of action of CXCR7 in renal fibrosis is unclear.

In addition, we unexpectedly found that CXCR7 inhibited the Wnt/ $\beta$ -catenin pathway and its downstream target proteins (Figure 7). In addition to its role in development, the Wnt/ $\beta$ -catenin pathway functionally contributes to fibrosis in several organs [24].

A previous study showed that the expression of CXCR7 was controlled by the restriction of Wnt/ $\beta$ -catenin signaling; conversely, CXCR7 inhibited the  $\beta$ -catenin-dependent induction of Jag1 to ameliorate fibrosis, indicating that the CXCR7 and Wnt/ $\beta$ -catenin pathways might be functionally linked [18, 20]. In our study, we confirmed that CXCR7 inhibited EMT *via* the Wnt/ $\beta$ -catenin pathway. However, we were unable to determine a direct correlation between CXCR7 and  $\beta$ -catenin signaling.

The  $\beta$ -catenin pathway is pivotal for controlling myriad biological phenomena throughout the developmental life of all animals. As a developmental pathway,  $\beta$ -catenin signaling is silent in adult kidneys but is reactivated in a variety of nephropathies [18, 24,25]. However, the specific relationships between CXCR7 and  $\beta$ -catenin are unclear. In our study, we confirmed that CXCR7 inhibited renal fibrosis *via* the Wnt/ $\beta$ -catenin pathway. However, this mechanism remains elusive and warrants future study.

Collectively, these results highlight that CXCR7 may be a new therapeutic target for CKD. While promising work has been done to investigate the effects of CXCR7, this has been performed only in animal models. However, no clinical trials on the use of CXCR7 for kidney disease have been performed. However, clinical data are needed to further understand the role of CXCR7 in this disease.

## Conclusions

Overall, we showed that CXCR7 plays an important role in renal fibrosis. CXCR7 is significantly downregulated in tubular cells. Additionally, activation of CXCR7 can block renal fibrosis through the  $\beta$ -catenin signaling pathway. This study identified a novel target for inhibiting the process of renal fibrosis. Thus, these results provide proof-of-principle that targeted activation of tubular CXCR7 could constitute a novel therapeutic approach for renal fibrosis.

## Authors' contributions

Ping Meng contributed to the conceptualization and methodology of this study and drafted the original manuscript. Chunli Liu and Jingchun Li contributed to the validation and visualization of the data. Ping Fang and Bo Yang contributed to the analysis and interpretation of the data. Yunfang Zhang and Wei Sun contributed to the supervision of the data and the review and editing of the manuscript. All the authors have read and approved the final manuscript.

## Disclosure statement

The authors declare that they have no conflict of interest.

## Funding

This work was supported by the Guangzhou Health Science and Technology project (20221A011115), the National Natural Science Foundation of China (82300760), the Key Medical Discipline of Guangzhou (2021-2023), the Huadu District Basic and Applied Basic Research Joint Funded Project (23HDQYLH01), the Guangzhou Science and Technology project (202102021296) and the Guangdong Medical Research Foundation (A2021251).

## Data availability statement

The raw data supporting the conclusions of this article will be made available by the authors without undue reservation.

## References

- [1] Carney EF. The impact of chronic kidney disease on global health. *Nat Rev Nephrol.* 2020;16(5):1–13. doi:10.1038/s41581-020-0268-7.
- [2] Huang R, Fu P, Ma L. Kidney fibrosis: from mechanisms to therapeutic medicines. *Sig Transduct Target Ther.* 2023;8(1):129. doi:10.1038/s41392-023-01379-7.
- [3] Lanzon B, Martin-Taboada M, Castro-Alves V, et al. Lipidomic and metabolomic signature of progression of chronic kidney disease in patients with severe obesity. *Metabolites.* 2021;11(12):836. doi:10.3390/metabo11120836.
- [4] Hughes CE, Nibbs R. A guide to chemokines and their receptors. *Febs J.* 2018;285(16):2944–2971. doi:10.1111/febs.14466.
- [5] Wu F, Sun C, Lu J. The role of chemokine receptors in renal fibrosis. *Rev Physiol Biochem Pharmacol.* 2020;177:1–24. doi:10.1007/112\_2020\_21.
- [6] Liu P, Li X, Lv W, et al. Inhibition of CXCL1-CXCR2 axis ameliorates cisplatin-induced acute kidney injury by mediating inflammatory response. *Biomed Pharmacother.* 2020;122:109693. doi:10.1016/j.biopha.2019.109693.
- [7] Meng P, Huang J, Ling X, et al. CXCR2 accelerates tubular cell senescence and renal fibrosis via  $\beta$ -Catenin-induced mitochondrial dysfunction. *Front Cell Dev Biol.* 2022;10:862675. doi:10.3389/fcell.2022.862675.
- [8] Wang D, Chen X, Fu M, et al. Tacrolimus increases the expression level of the chemokine receptor CXCR2 to promote renal fibrosis progression. *Int J Mol Med.* 2019;44(6):2181–2188. doi:10.3892/ijmm.2019.4368.
- [9] Liu Y, Feng Q, Miao J, et al. C-X-C motif chemokine receptor 4 aggravates renal fibrosis through activating JAK/STAT/GSK3 $\beta$ /beta-catenin pathway. *J Cell Mol Med.* 2020;24(7):3837–3855. doi:10.1111/jcmm.14973.
- [10] Mo H, Ren Q, Song D, et al. CXCR4 induces podocyte injury and proteinuria by activating beta-catenin signaling. *Theranostics.* 2022;12(2):767–781. doi:10.7150/thno.65948.
- [11] Mo H, Wu Q, Miao J, et al. C-X-C chemokine receptor type 4 plays a crucial role in mediating oxidative Stress-Induced podocyte injury. *Antioxid Redox Signal.* 2017;27(6):345–362. doi:10.1089/ars.2016.6758.
- [12] Wu Y, An C, Jin X, et al. Disruption of CXCR6 ameliorates kidney inflammation and fibrosis in deoxycorticosterone acetate/salt hypertension. *Sci Rep.* 2020;10(1):133. doi:10.1038/s41598-019-56933-7.
- [13] Xia Y, Jin X, Yan J, et al. CXCR6 plays a critical role in angiotensin II-induced renal injury and fibrosis. *Arterioscler Thromb Vasc Biol.* 2014;34(7):1422–1428. doi:10.1161/ATVBAHA.113.303172.
- [14] Lounsbury N. Advances in CXCR7 modulators. *Pharmaceuticals (Basel).* 2020;13(2):33. doi:10.3390/ph13020033.
- [15] Wang C, Chen W, Shen J. CXCR7 targeting and its major disease relevance. *Front Pharmacol.* 2018;9:641. doi:10.3389/fphar.2018.00641.
- [16] Guan S, Zhou J. CXCR7 attenuates the TGF- $\beta$ -induced endothelial-to-mesenchymal transition and pulmonary fibrosis. *Mol Biosyst.* 2017;13(10):2116–2124. doi:10.1039/c7mb00247e.
- [17] Shi A, Wang T, Jia M, et al. Effects of SDF-1/CXCR7 on the migration, invasion and epithelial-Mesenchymal transition of gastric cancer cells. *Front Genet.* 2021;12:760048. doi:10.3389/fgene.2021.760048.



- [18] Cao Z, Lis R, Ginsberg M, et al. Targeting of the pulmonary capillary vascular niche promotes lung alveolar repair and ameliorates fibrosis. *Nat Med*. 2016;22(2):154–162. doi:[10.1038/nm.4035](https://doi.org/10.1038/nm.4035).
- [19] Menhaji-Klotz E, Hesp KD, Londregan AT, et al. Discovery of a novel small-Molecule modulator of C-X-C chemokine receptor type 7 as a treatment for cardiac fibrosis. *J Med Chem*. 2018;61(8):3685–3696. doi:[10.1021/acs.jmedchem.8b00190](https://doi.org/10.1021/acs.jmedchem.8b00190).
- [20] Shen M, Feng Y, Wang J, et al. CXCR7 inhibits fibrosis via wnt/beta-Catenin pathways during the process of angiogenesis in human umbilical vein endothelial cells. *Biomed Res Int*. 2020;2020:1216926–1216910. doi:[10.1155/2020/1216926](https://doi.org/10.1155/2020/1216926).
- [21] Zhou L, Zhou S, Yang P, et al. Targeted inhibition of the type 2 cannabinoid receptor is a novel approach to reduce renal fibrosis. *Kidney Int*. 2018;94(4):756–772. doi:[10.1016/j.kint.2018.05.023](https://doi.org/10.1016/j.kint.2018.05.023).
- [22] Kim KK, Sheppard D, Chapman HA. TGF-beta1 signaling and tissue fibrosis. *Cold Spring Harb Perspect Biol*. 2018;10(4):a022293. doi:[10.1101/cshperspect.a022293](https://doi.org/10.1101/cshperspect.a022293).
- [23] Humphreys BD. Mechanisms of renal fibrosis. *Annu Rev Physiol*. 2018;80(1):309–326. doi:[10.1146/annurev-physiol-022516-034227](https://doi.org/10.1146/annurev-physiol-022516-034227).
- [24] Schunk SJ, Floege J, Fliser D, et al. WNT-beta-catenin signalling - a versatile player in kidney injury and repair. *Nat Rev Nephrol*. 2021;17(3):172–184. doi:[10.1038/s41581-020-00343-w](https://doi.org/10.1038/s41581-020-00343-w).
- [25] Nlandu-Khodo S, Osaki Y, Scarfe L, et al. Tubular beta-catenin and FoxO3 interactions protect in chronic kidney disease. *JCI Insight*. 2020;5(10):e135454. doi:[10.1172/jci.insight.135454](https://doi.org/10.1172/jci.insight.135454).